Quaternary Geochronology 50 (2019) 1–7

Contents lists available at ScienceDirect

Quaternary Geochronology

journal homepage: www.elsevier.com/locate/quageo

In-situ garnet ^{238}U-^{230}Th geochronology of Holocene silica-undersaturated volcanic tuffs at millennial-scale precision

Jörn-Frederik Wotzlaw[a,*], Marcel Guillong[a], Anna Balashova[a], Francesca Forni[a,b], István Dunkl[c], Hannes B. Mattsson[a,d], Olivier Bachmann[a]

[a] Institute of Geochemistry and Petrology, Department of Earth Sciences, ETH Zurich, Zurich, Switzerland
[b] Earth Observatory of Singapore, Nanyang Technological University, Singapore
[c] Sedimentology and Environmental Geology, University of Göttingen, Göttingen, Germany
[d] Department of Earth Sciences, Uppsala University, Uppsala, Sweden

ARTICLE INFO

Keywords:
U-Th geochronology
Magmatic garnet
LA-ICPMS
Vesuvius
Oldoinyo Lengai
Hominin footprints

ABSTRACT

Radioisotopic dates for Late Pleistocene to Holocene silica-undersaturated volcanic rocks are often imprecise, limiting our ability to assess the frequency of eruptions in alkaline volcanic provinces, evaluate related volcanic risk and date associated archaeological sites. Here, we present a new approach to dating alkaline volcanic rocks employing ^{238}U-^{230}Th disequilibrium dating of Ca-rich garnet phenocrysts by laser ablation inductively coupled plasma mass spectrometry (LA-ICPMS). We document analytical protocols and apply this technique to date magmatic garnets from the 472 AD Pollena eruption of Vesuvius (Southern Italy) and from the Engare Sero Footprint Tuff, a volcaniclastic unit attributed to Oldoinyo Lengai (Northern Tanzania). Garnet phenocrysts from the Pollena phonolite yield a well-defined U-Th isochron with a date of 2.28 ± 0.71 ka (1σ) that is indistinguishable from the historical date and suggests that garnet crystallized close to eruption with a pre-eruption residence time of less than 1.6 kyr. Garnets from the Engare Sero Footprint Tuff yield a U-Th isochron date of 4.91 ± 0.58 ka (1σ). This date is compatible with ^{14}C and ^{40}Ar/^{39}Ar dates that bracket tuff deposition to between ~5 and ~19 ka but confidently constrains the age of the Engare Sero Footprint Tuff to the mid-Holocene. These examples demonstrate the potential of this new approach for dating Late Pleistocene to Holocene silica-undersaturated volcanic rocks at millennial-scale precision and for investigating magma chamber processes beneath active alkaline volcanoes.

1. Introduction

Precise and accurate geochronology of Quaternary volcanic rocks is most commonly achieved by using the ^{40}Ar/^{39}Ar technique (McDougall and Harrison, 1999). However, ^{40}Ar/^{39}Ar dating of Pleistocene to Holocene silica-undersaturated volcanic rocks is often limited to K-rich groundmass because K-rich phenocrysts common in these rocks (e.g. biotite, phlogopite, feldspathoids) frequently contain excess-Ar (Lippolt et al., 1990; Renne, 1995; McDougall and Harrison, 1999; Kelley, 2002; Hora et al., 2010). Due to the high Zr solubility in alkaline melts, these rocks typically also lack accessory zircon that would allow U-Pb, U-Th and/or (U-Th)/He dating (e.g. Condomines, 1997; Schmitt, 2006; Danišík et al., 2016). These limitations result in often imprecise and/or inaccurate dates for Pleistocene to Holocene silica-undersaturated lavas and pyroclastic rocks.

Ca-rich garnet of the grossular-andradite series is a prominent mineral in contact metamorphic skarns and hydrothermally altered rocks (Russell et al., 1999) but is also a relatively common mineral in silica-undersaturated volcanic and plutonic rock (Stoppa and Lavecchia, 1992; Russell et al., 1999; Stoppa et al., 2002; Aciego et al., 2003; Scheibner et al., 2007, 2008). Grossular-andradite garnets typically contain U and Th at the 1–100 ppm level, prompting several studies to evaluate the suitability of these garnets as a geochronometer using the (U-Th)/He, U-Th and U-Pb methods (Aciego et al., 2003; Scheibner et al., 2008; Seman et al., 2017). While the U-Pb method is suitable to date garnet from older skarns and intrusions (e.g., Seman et al., 2017; Gevedon et al., 2018), the U-Th and (U-Th)/He methods can be used to date garnet from Pleistocene to Holocene volcanic deposits to assess their eruption ages and pre-eruption magma residence times (Aciego et al., 2003; Scheibner et al., 2008).

Here, we present a new approach to dating garnet phenocrysts from phonolitic to nephelinitic volcanic rocks employing ^{238}U-^{230}Th

* Corresponding author.
E-mail address: joern.wotzlaw@erdw.ethz.ch (J.-F. Wotzlaw).

https://doi.org/10.1016/j.quageo.2018.10.004
Received 29 July 2018; Received in revised form 22 September 2018; Accepted 23 October 2018
Available online 01 November 2018
1871-1014/

disequilibrium dating by laser ablation inductively coupled plasma mass spectrometry (LA-ICPMS). We document analytical protocols, data reduction procedures and apply this technique to date garnets from two Holocene volcanic eruption, the 472 AD Pollena eruption of Vesuvius (southern Italy, Rosi and Santacroce, 1983; Mastrolorenzo et al., 2002) and the Engare Sero Footprint Tuff (ESFT), a nephelinitic volcaniclastic unit derived from Oldoinyo Lengai volcano, Tanzania (Balashova et al., 2016; Liutkus-Pierce et al., 2016).

2. Materials and analytical methods

2.1. Sample preparation

Tuff samples were gently crushed, sieved and washed in deionized water. Garnets were handpicked from the < 2 mm sieve fractions. Selected crystals were sonicated in 8% HF for 2 min to remove adhering matrix and subsequently rinsed and sonicated with deionized water. Crystals were mounted in epoxy resin, polished to expose crystal interiors and imaged using back scattered electron imaging employing a scanning electron microscope and analysed for major element concentrations using a JEOL JXA-8200 electron microprobe at ETH Zurich. A separate set of ESFT garnets was mounted in epoxy resin to expose outermost crystal faces without polishing, allowing analysis of the outermost growth zones by depth-profiling. Glass reference materials and garnets that are inferred to be in secular U-series equilibrium based on independent age constraints were mounted in separate epoxy mounts and polished for analysis.

2.2. U-Th isotopic measurements

U-Th isotopic measurements were performed by LA-ICPMS using an Australian Scientific Instruments Resolution 155 laser ablation system coupled with a Thermo Element XR sector field ICPMS at the Institute of Geochemistry and Petrology of ETH Zurich. The analytical approach was adopted from methods developed for zircon U-Th dating (Guillong et al., 2016). The details of these methods and modifications required to analyse garnet are outlined below. Specific operating conditions are listed in Table 1. The laser was operated with an energy density of 3.5 J cm^{-2}, a repetition rate to 10 Hz and ablation spot sizes of either 173 or 257 µm diameter. Masses 230 and 235 were measured in pulse counting mode and masses 232 and 238 were measured in analogue mode. Measured ^{230}Th count rates were corrected for counts from the peak tail of ^{232}Th using the abundance sensitivity determined from a high-Th monazite ablated with 13 or 20 µm laser crater (average abundance sensitivity = 1.81 ppm; see Guillong et al., 2016 for details). Instrumental mass bias was determined from the measured ^{238}U/^{235}U relative to the natural U isotopic ratio of 137.818 (Hiess et al., 2012). To our knowledge, there are no garnet reference materials that are homogeneous in U and Th concentration and U/Th. We therefore tested two different approaches to determine a relative sensitivity factor (RSF) to correct for differences in sensitivity between U and Th. The first one uses a non-matrix matched correction based on the U/Th of measured reference glasses (NIST612, TB1G, GSD-1G and BCR2G). The second approach uses the Mali garnet (202.0 ± 1.2 Ma, Seman et al., 2017) as the primary reference material assuming (^{230}Th)/(^{238}U) = 1 to

Table 1
Instrumentation, operating conditions, data acquisition parameters and data reduction.

Laboratory and Sample Preparation	
Laboratory name	Department of Earth Sciences, ETH Zurich
Sample type/mineral	garnet
Sample preparation	Crushed, hand-picked from < 1 mm sieve fraction, epoxy mounted, 1 µm polish
Laser ablation system	
Make, Model & type	Australian Scientific Instruments Resolution 155
Ablation cell & volume	Laurin Technics 155, constant geometry, aerosol dispersion volume < 1 cm^3
Laser wavelength	193 nm
Pulse width	25 ns
Energy density/Fluence	~3.5 J cm^{-2}
Repetition rate	10 Hz
Spot size	173 µm (257 µm for VC-1, 13 or 20 µm for monazite)
Ablation rate	~50 nm pulse^{-1}
Sampling mode/pattern	Single hole drilling, 3 cleaning pulses
Carrier gas and flow	100% He, 0.5 l min^{-1}
Ablation duration	50 s
ICP-MS Instrument	
Make, Model & type	Thermo Element XR SF-ICP-MS
Sample introduction	Ablation aerosol only, squid aerosol homogenization device
RF power	1550 W
Make-up gas flow	~0.95 l min^{-1} Ar (gas mixed to He carrier inside ablation cell funnel)
Detection system	Single detector triple mode SEM, analogue, Faraday
Masses monitored	230, 232, 235, 238 amu
Integration time per peak	150 ms (mass 230), 25 ms (mass 235), 20 ms (mass 232 analogue), 10 ms (mass 238 analogue)
Total integration time per reading	0.205 s of 0.2145 s reading time, 0.0095 s settling time per reading
Dead time	24 ns
Typical oxide rate (ThO/Th)	0.18% (NIST 612, 43 µm, 10 Hz)
Typical doubly charged rate (Ba^{++}/Ba^{+})	3.50% (NIST 612, 43 µm, 10 Hz)
Data Processing	
Gas blank	40 s prior to each ablation spot
Calibration strategy	Secular equilibrium of Mali garnet used to correct for mass bias and differences in sensitivity between U and Th.
Reference Material information	Mali garnet (202.0 ± 1.2 Ma, Seman et al., 2017), assuming (^{230}Th)/(^{238}U) = 1
Data processing package used	SILLS (Guillong et al., 2008), Excel and IsoplotR (Vermeesch, 2018).
Mass discrimination	Mass bias correction for all ratios normalized to natural ^{238}U/^{235}U of 137.818 (Hiess et al., 2012)
Uncertainty level & propagation	^{230}Th counts, ratios and dates are given as combined standard uncertainty.
Quality control/Validation	Based on garnets in secular equilibrium (Fig. 1A)

determine the RSF from the isotopic ratio. The RSF determined from reference glasses is on average 15% higher than the one determined from the secular equilibrium garnet when tuned for maximum sensitivity implying a significant matrix effect. This matrix effect can be reduced by changing the ICP parameters but this results in a significant loss of sensitivity. As counting statistics, i.e. the number of counts on ^{230}Th, is the primary source of uncertainty, we prefer the matrix-matched approach that allows tuning for maximum sensitivity to optimize the count rate on ^{230}Th. The accuracy of this correction procedure was evaluated by analysing secular equilibrium garnets of various composition including the 35 ± 2 Ma Lake Jaco grossular (Seman et al., 2017), ~27 Ma grossular-andradite garnets from the Karavansalija Mineralised Centre, Rogozna Mountains, SW Serbia (I. Peytcheva, unpublished data), and a magmatic spessartine-almandine garnet (VC-1) associated with the ~40 Ma Bruffione granodiorite in the southern Adamello batholith (Zhang et al., 2001). U-Th isotopic data for all garnet reference materials and unknowns are provided in Supplementary Table 1.

2.3. (U-Th)/He geochronology

Selected euhedral garnet crystals from the ESFT were also dated using (U-Th)/He techniques at the Thermochronology Lab of the Geoscience Centre at the University of Göttingen. Single or double-crystal aliquots were wrapped in platinum capsules and heated in the full-metal extraction line by an infra-red laser for 2 min in high vacuum. After gettering the noble gases were expanded into a Hiden triple-filter quadrupole mass spectrometer equipped with a positive ion counting detector. Crystals were checked for incomplete degassing of He by sequential reheating and He measurement. The amount of He extracted in the second runs was usually around 1%. Following degassing, samples were retrieved from the gas extraction line, loaded in teflon dissolution vessels, spiked with calibrated ^{230}Th and ^{233}U solutions and dissolved in pressurized teflon bombs using a mixture of double distilled 48% HF and 65% HNO_3. Each sample batch was prepared with a series of procedural blanks and spiked normals to check the purity and calibration of the reagents and spikes. Spiked solutions were analysed using a Thermo iCAP Q ICP-MS. Procedural U and Th blanks of this method are usually very stable and below 1 pg. Concentrations of Ca and Sm were measured by external calibration. The ejection correction factors (Ft; Farley et al., 1996) were determined assuming an oblate spheroid that follows the shape of the multifaceted, euhedral to slightly irregular garnet crystals. The (U-Th)/He data are provided in Table 2.

3. Results and discussion

3.1. Secular equilibrium garnets

Garnets older than ~350,000 years are assumed to be in secular U-series equilibrium in which the number of decays per unit time (i.e. the activity) is equal for all parent and intermediate daughter isotopes. Analysed secondary reference garnets are heterogeneous with respect to U, Th and Th/U (Supplementary Table 1; Fig. 1A) but yield abundance sensitivity and RSF corrected (^{230}Th)/(^{238}U) consistent with secular equilibrium (Fig. 1A). Uncertainties on corrected (^{230}Th)/(^{238}U) ratios are dominated by counting statistics on the least abundant isotope ^{230}Th with minor contributions from the abundance sensitivity and RSF corrections. Uncertainties on (^{230}Th)/(^{238}U) are therefore tightly correlated with U concentration (Fig. 1B). While accuracy does not seem to be significantly compromised at lower concentration, analytical precision is strongly controlled by U concentration and corresponding ^{230}Th count rate (Fig. 1B). However, uncertainties on U-Th isochron dates additionally depend on the spread in (^{238}U)/(^{232}Th) and meaningful data can be obtained essentially for all garnets with ^{230}Th above detection limit (Fig. 1B).

3.2. Application to Late Pleistocene to Holocene volcanic tuffs

3.2.1. Pollena phonolite

The 472 AD Pollena eruption marked the reawakening of Somma-Vesuvius after a couple of centuries of quiescence and represents one of the largest sub-Plinian events in the history of the volcano (Cioni et al., 2008). The eruption is mentioned in several historical documents of Byzantine chroniclers (e.g. Marcellinus *Comes*) providing evidence that ash clouds associated with this eruption reached as far as Constantinople (Rosi and Santacroce, 1984; Principe et al., 2004). The pyroclastic succession associated with the Pollena eruption consist of a basal fallout sequence of pumice and coarse ash followed by massive and dune-bedded deposits of pyroclastic density currents (PDC) alternating with minor fallout layers (Rosi and Santacroce, 1983; Rolandi et al., 2004; Sulpizio et al., 2005). The PDC deposits crop out mainly in the northern and south-eastern flanks of the old volcanic edifice that collapsed after the 79 AD eruption of Pompei (Somma caldera; Fig. 2A) while ash fall deposits are found for several 10s of km to the north-east of Somma-Vesuvius (Sulpizio et al., 2005). The juvenile components range in composition from tephri-phonolites to phonolites and typically contain abundant leucite and clinopyroxene with minor sanidine, nepheline, biotite and garnet (Santacroce et al., 2008).

Table 2
(U-Th)/He isotopic data for Engare Sero Footprint Tuff garnets.

Sample	^{4}He[a]		^{238}U[b]		^{232}Th[b]		Sm[b]		Ejection	Uncorr.	Corr.	
	vol.	1σ	mass	1σ	mass	1σ	mass	1σ	correct.	He date	He date	2σ
	[ncc]	[%]	[ng]	[%]	[ng]	[%]	[ng]	[%]	(Ft)[c]	[Ma][d]	[Ma][e]	[Ma][e]
FT14–16.1	0.058	2.7	1.078	1.8	1.652	2.4	12.244	6.9	0.897	0.303	0.338	0.023
FT14–16.2	0.050	2.8	1.299	1.8	2.266	2.4	15.213	6.8	0.897	0.211	0.235	0.016
FT14–16.3	0.210	1.8	1.236	1.8	1.843	2.4	15.103	6.8	0.898	0.970	1.081	0.059
FT14–16.5	0.075	2.3	0.844	1.8	1.285	2.4	11.757	6.7	0.919	0.502	0.546	0.033
FT14–16.6	0.104	2.0	0.733	1.8	0.668	2.4	8.926	6.9	0.895	0.894	0.999	0.058
FT14–16.7	0.004	8.2	0.609	1.8	0.802	2.4	7.805	6.8	0.889	0.035	0.040	0.007
FT14–16.8	0.026	3.5	0.513	1.8	1.288	2.4	6.586	6.8	0.863	0.243	0.282	0.024
FT14–16.9	0.108	2.1	0.814	1.8	1.419	2.4	11.384	6.8	0.871	0.718	0.824	0.052

[a] Amount of helium is given in nano-cubic-cm in standard temperature and pressure.
[b] Amount of radioactive elements are given in nanograms.
[c] Ejection correction (Ft): correction factor for alpha-ejection assuming an oblate ellipsoid.
[d] Uncorrected for alpha ejection.
[e] Corrected for alpha ejection, uncertainties are given as 2s and include analytical and Ft uncertainties.

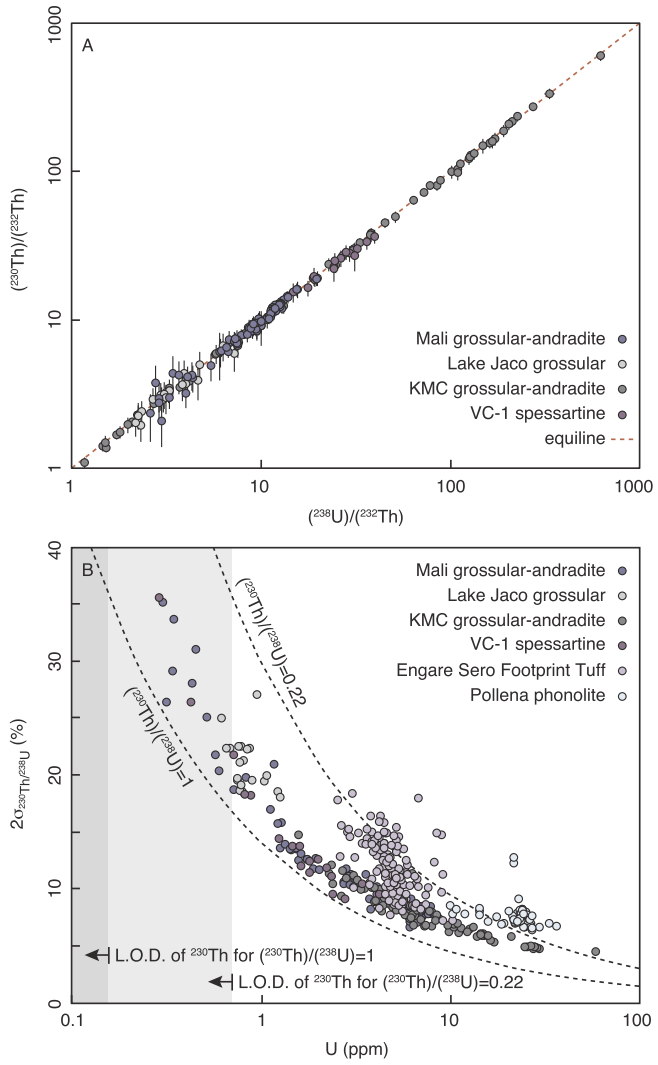

Fig. 1. U-Th isotope systematics of analysed secular equilibrium garnets. (A) U-Th isochron diagram displaying the abundance sensitivity and RSF corrected U-Th isotopic compositions of secular equilibrium garnets. Data point uncertainties are 2σ. (B) Analytical uncertainty of corrected $^{230}Th/^{238}U$ activity ratios as a function of U concentration. Dotted lines are the theoretical limits based on counting statistics with ^{230}Th counts translated into U concentration for two different activity ratios using the average Th sensitivity and a total integration time of 30 s.

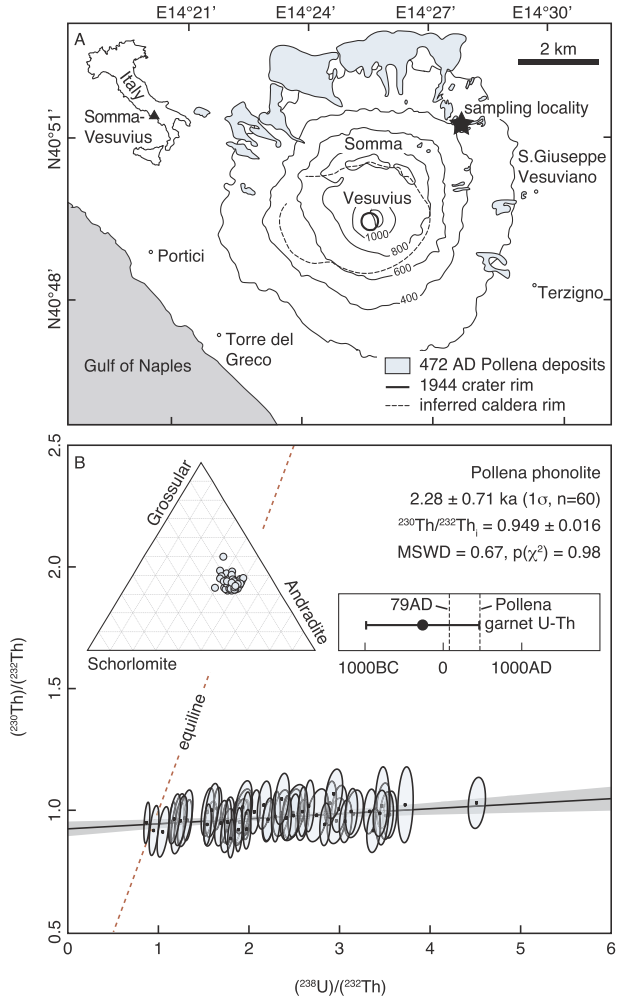

Fig. 2. Sampling locality and U-Th isotope systematics of garnet phenocrysts from the Pollena eruption of Mount Vesuvius. (A) Map of the Somma-Vesuvius volcanic complex displaying the distribution of PDC deposits associated with the 472 AD Pollena eruption (after Sulpizio et al., 2007). Black star marks the sample locality. (B) U-Th isochron for garnets from pumices of the Pollena phonolite. Data point uncertainties are 2σ. Insets show the major element composition of analysed garnets and a comparison of the garnet U-Th date with the historical date.

We separated garnet from pumiceous clasts collected along a stratigraphic sequence exposed on the north-eastern slope of the Somma-Vesuvius volcanic complex. The sampled stratigraphic units correspond to the fallout layers L1, L4, L7 and L8 described by Sulpizio et al. (2005; see Supplementary Table 1). Analysed garnets are grossular-andradite solid solutions and are rather homogeneous in major element composition (see inset in Fig. 2B and Supplementary Table 2). U concentrations in analysed Pollena garnets range from 10.0 to 36.6 ppm, Th concentrations from 14.4 to 119 ppm and Th/U from 0.8 to 4.0. U-Th isotopic data yield a well-defined isochron with a date of 2.28 ± 0.71 ka (1σ, n = 60, MSWD = 0.67) and an initial $(^{230}Th)/(^{232}Th)$ of 0.949 ± 0.016 (Fig. 2B).

The ^{238}U-^{230}Th date is indistinguishable from the historical age suggesting that these garnets crystallized close to eruption with a limited pre-eruption residence time of less than 1.6 kyr. This residence time is shorter than the residence time of garnets from the 8.89 ka Plinian Mercato eruption (Scheibner et al., 2008). Overall, this data demonstrates that garnet U-Th dating can provide accurate eruption ages for Holocene tephras and insights into the pre-eruption crystallization history of silica-undersaturated magmas.

3.2.2. Engare Sero Footprint Tuff

The Engare Sero Footprint Tuff (ESFT) is a nephelinitic volcaniclastic unit exposed at the south-western shore of Lake Natron in Northern Tanzania (Balashova et al., 2016; Liutkus-Pierce et al., 2016: Fig. 3). Balashova et al. (2016) subdivided the tuffaceous unit into a lower and upper subunit while Liutkus-Pierce et al. (2016) further distinguished two members in the lower subunit that are separated by a clay layer. The lower subunit contains abundant mammal footprints including those of *Homo sapiens* providing a snapshot of the environment in which these modern humans lived and evolved (Balashova et al., 2016; Liutkus-Pierce et al., 2016). Since its discovery, the age and origin of this volcaniclastic unit have been under debate despite the importance of accurate and precise age constraints for placing this snapshot into a larger framework of regional climate and landscape

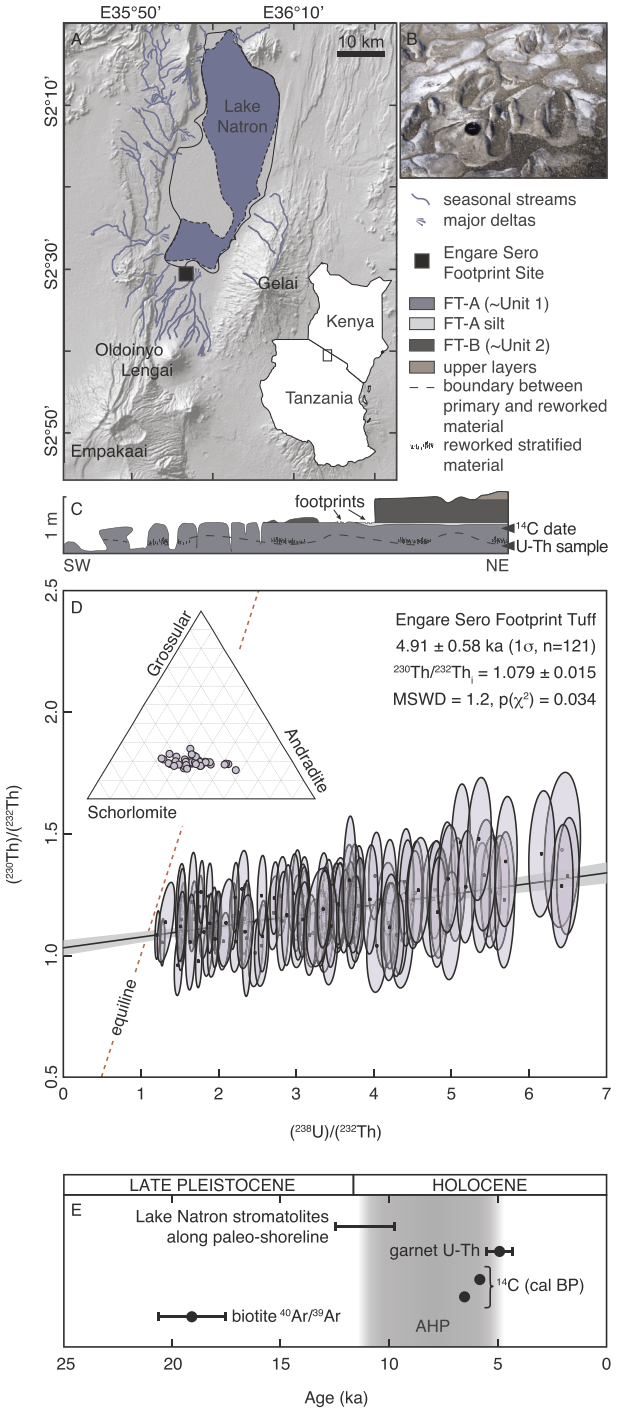

Fig. 3. Geological and stratigraphic framework of the Engare Sero Footprint Tuff and U-Th isotope systematics of analysed garnets. (A) Map of the northern Tanzanian sector of the Gregory Rift displaying the location of the Engare Sero Footprint Site south of Lake Natron and selected volcanoes in the close vicinity (modified from Balashova et al., 2016). (B) Outcrop photograph showing hominin footprints in the tuff. Lens cap for scale. (C) Stratigraphic sketch of the Engare Sero Footprint Tuff according to Balashova et al. (2016) showing the relationship between the unit sampled for garnet U-Th geochronology and the layer containing gastropod shells dated by ^{14}C geochronology by Liutkus-Pierce et al. (2016). (D) U-Th isochron for garnets from the Engare Sero Footprint Tuff. Data point uncertainties are 2σ. Inset shows the major element composition of analysed garnets. (E) Comparison of our garnet U-Th date with ^{40}Ar/^{39}Ar biotite and ^{14}C dates (Liutkus-Pierce et al., 2016) of the ESFT and ^{14}C dates of Lake Natron paleo-shoreline stromatolites (Hillaire-Marcel et al., 1986). Also shown is the temporal extent of the Holocene African Humid Period (AHP).

evolution. We separated garnet crystals from the footprint-bearing lower subunit (FT-A of Balashova et al., 2016) for U-Th geochronology. Analysed garnets are titanian andradites (Fig. 3) with U concentrations ranging from 2.6 to 10.4 ppm, Th concentrations between 1.4 and 29.8 ppm and Th/U between 0.5 and 2.9 (Supplementary Table 1). Analyses of the outermost crystal faces reveals the presence of thin high-Th and high-Th/U rims on some garnets. However, they are analytically indistinguishable in terms of U-Th isotope systematics from crystal interiors and we therefore include all analyses into a single isochron. The U-Th isotopic data of 121 spot analyses yield a well-defined isochron with a date of 4.91 ± 0.58 ka (1σ, n = 121, MSWD = 1.2) and an initial (^{230}Th)/(^{232}Th) of 1.079 ± 0.015.

Liutkus-Pierce et al. (2016) reported conventional ^{14}C dates of 5.135 ± 0.030 and 5.760 ± 0.030 ka BP for gastropod shells from the footprint-bearing stratigraphic level. For comparison with our garnet U-Th dates we calibrated these ^{14}C dates employing the SHCal13 calibration (Hogg et al., 2013; Stuiver et al., 2018) yielding 95% confidence ranges of 5.746–5.915 cal ka BP and 6.412–6.631 cal ka BP, respectively. Our U-Th isochron date is indistinguishable from the younger of the two ^{14}C dates but is distinct from the older date (Fig. 3). However, our garnet U-Th date is significantly younger than biotite ^{40}Ar/^{39}Ar dates also reported by Liutkus-Pierce et al. (2017; Fig. 3). The youngest biotite ^{40}Ar/^{39}Ar date of 19.1 ± 3.1 ka provides a maximum age that permits a Late Pleistocene age for the ESFT (Liutkus-Pierce et al., 2016). This age discordance may be partly due to excess-Ar in biotite (e.g. Kelley, 2002; Bachmann et al., 2010; Hora et al., 2010). However, biotite crystals are present only in the upper part of the ESFT and display abraded edges due to aeolian or fluvial reworking of loose ash (Balashova et al., 2016, Liutkus-Pierce et al., 2016). With Oldoinyo Lengai being the most likely source of the ESFT and biotite being absent in Oldoinyo Lengai magmas, biotites are considered xenocrystic in the ESFT. Incorporation of older biotites therefore likely also contributes to the age discordance between ^{40}Ar/^{39}Ar dates and garnet U-Th dates. In contrast, the excellent agreement between our garnet U-Th date and the younger of two ^{14}C dates reported by Liutkus-Pierce et al. (2016) confidently places the deposition age of the ESFT into the mid-Holocene (Fig. 3). This is consistent with the ESFT post-dating the Late Pleistocene to Early Holocene lake level highstand of Lake Natron (Hillaire-Marcel et al., 1986) and with regional stratigraphic correlations presented by Balashova et al. (2016). The ESFT therefore provides a snapshot of the interaction of modern humans with a volcanically influenced dynamic environment across the termination of the Holocene African Humid Period (Fig. 3).

In contrast to the well-defined U-Th date, (U-Th)/He dates of selected ESFT garnets range from 0.040 ± 0.007 to 1.081 ± 0.059 Ma (Table 2) therefore significantly pre-dating eruption. We attribute this age discordance to significant excess-He trapped in these garnets either in the crystal lattice or in inclusions. As the garnets are non-transparent, it is difficult to assess the influence of inclusions in He-dated crystals, however, we frequently observed mineral inclusions (primarily nepheline) in crystal interiors of polished garnets prepared for U-Th dating. The discordance between our U-Th and (U-Th)/He dates is significantly different to garnets from the 79 AD eruption of Somma-Vesuvius dated by (U-Th)/He by Aciego et al. (2003) that did not contain any resolvable excess-He and yielded dates in agreement with the historical age. Interestingly, in the East African Rift, particularly the Tanzanian sector of the Gregory Rift, volcanic fumaroles contain high amount of He with ^{3}He/^{4}He ratios characteristic of a sub-continental lithospheric mantle source (e.g., Teague et al., 2008; Mollex et al., 2018) while He-rich gas seeps with crustal He-isotope signatures sample some of world's largest sub-surface ^{4}He reservoirs (Danabalan et al., 2016). However, explaining the excess-He and resulting age discordance with high-He host magma requires a mechanism for incorporation and retention of He in analysed garnets. Dunai and Roselieb (1996) studied and quantified sorption of helium in almandine-pyrope garnet. Assuming that Ca-rich garnets have similarly low

ionic porosity and therefore high closure temperature (see Aciego et al., 2003 and related comments for discussion), helium sorption during garnet growth from a magma with high He partial pressure may explain the observed age discordance. Excess-He, similar to excess-Ar, may therefore be prevalent in settings with high volatile flux from the mantle resulting in magmas with high Ar and He contents (e.g., Bachmann et al., 2010).

4. Summary and conclusions

We document a new approach to dating silica-undersaturated volcanic rocks using in situ ^{238}U-^{230}Th geochronology of magmatic Ca-rich garnet. Garnet phenocrysts from the 472 AD Pollena eruption of Vesuvius (Italy) and the nephelinitic Engare Sero Footprint Tuff (Lake Natron, Tanzania) yield well-defined internal U-Th isochrons with dates that agree with independent historical and radioisotopic age constraints. Due to the large variations in Th and U concentrations and resulting large spread in (^{238}U)/(^{232}Th), garnet U-Th isochron dates rival zircon U-Th and $^{40}Ar/^{39}Ar$ dates in terms of analytical precision with uncertainties of less than 1000 years for Holocene eruptions. In the cases we investigated, pre-eruption residence time of garnet is unresolvable and garnet U-Th dates yield accurate eruption ages but this may be different for larger phonolitic eruptions (Scheibner et al., 2008). Our garnet U-Th date for the Engare Sero Footprint Tuff confidently constrains the deposition age to the mid-Holocene therefore significantly improving the age estimate for this important volcaniclastic unit. In contrast, garnet (U-Th)/He dates from the same unit are significantly older than the U-Th date. We attribute this age discordance to significant excess-He in these garnet phenocrysts. Based on these examples, we anticipate that U-Th dating of magmatic garnet will provide important age constraints for several Late Pleistocene to Holocene silica-undersaturated volcanic units (e.g. from central and southern Italy and the East African Rift) and in combination with geochemical and isotopic analyses of the same crystals will provide important constraints on the pre-eruption storage and evolution of alkaline magmas.

Acknowledgements

We thank Peter Brack, Axel Gerdes and Irena Peytcheva for providing secular equilibrium garnets and Julien Allaz for his help with electron microprobe analyses. Alessandro Vona is acknowledged for providing samples of the Pollena eruption. We further thank Jorge Vazquez and an anonymous reviewer for constructive comments and David Richards for editorial handling.

Appendix A. Supplementary data

Supplementary data to this article can be found online at https://doi.org/10.1016/j.quageo.2018.10.004.

References

Aciego, S., Kennedy, B.M., DePaolo, D.J., Christensen, J.N., Hutcheon, I., 2003. U-Th/He age of phenocrysts garnet from the 79 AD eruption of Mt. Vesuvius. Earth Planet Sci. Lett. 219, 209–219.

Bachmann, O., Schoene, B., Schnyder, C., Spikings, R., 2010. The $^{40}Ar/^{39}Ar$ and U-Pb dating of young rhyolites in the Kos-Nisyros volcanic complex, Eastern Argean Arc, Greece: age discordance due to excess ^{40}Ar in biotite. G-cubed 11, Q0AA08.

Balashova, A., Mattsson, H.B., Hirt, A.M., Almqvist, B.S.G., 2016. The Lake Natron Footprint Tuff (northern Tanzania): volcanic source, depositional processes and age constraints from field relations. J. Quat. Sci. 31, 526–537.

Cioni, R., Bertagnini, A., Santacroce, R., Andronico, D., 2008. Explosive activity and eruption scenarios at Somma–Vesuvius (Italy): towards a new classification scheme. J. Volcanol. Geoth. Res. 178, 331–346.

Condomines, M., 1997. Dating recent volcanic rocks through 230Th–238U disequilibrium in accessory minerals: example of the Puy de Dôme (French Massif Central). Geology 25, 375–378.

Danabalan, D., Gluyas, J.G., Macpherson, C.G., Abraham-James, T.H., Bluett, J.J., Barry, P.H., Ballentine, C.J., 2016. New high-grade helium discoveries in Tanzania. Goldschmidt Abstracts 595.

Danišík, M., Schmitt, A., Stockli, D., Lovera, O., Dunkl, I., Evans, N., 2016. Application of combined U-Th-disequilibrium/U-Pb and (U-Th)/He zircon dating to tephrochronology. Quat. Geochronol. 40, 23–32.

Dunai, T.J., Roselieb, K., 1996. Sorption and diffusion of helium in garnet: implications for volatile tracing and dating. Earth Planet Sci. Lett. 139, 411–421.

Farley, K.A., Wolf, R.A., Silver, L.T., 1996. The effects of long alpha-stopping distances on (U-Th)/He ages. Geochem. Cosmochim. Acta 60, 4223–4229.

Gevedon, M., Seman, S., Barnes, J.D., Lackey, J.S., Stockli, D.F., 2018. Unraveling histories of hydrothermal systems via U-Pb laser ablation dating of skarn garnet. Earth Planet Sci. Lett. 498, 237–246.

Guillong, M., Meier, D.L., Allan, M.M., Heinrich, C.A., Yardley, B.W.D., 2008. SILLS: a MATLAB-based program for the reduction of laser ablation ICP-MS data of homogeneous materials and inclusions. Mineralogical Association of Canada Short Course 40, 328–333.

Guillong, M., Sliwinski, J.T., Schmitt, A.K., Forni, F., Bachmann, O., 2016. U-Th zircon dating by laser ablation single collector inductively coupled plasma-mass spectrometry (LA-ICP-MS). Geostand. Geoanal. Res. https://doi.org/10.1111/j.1751-908X.2016.00396.x.

Hiess, J., Condon, D.J., McLean, N., Noble, S.R., 2012. $^{238}U/^{235}U$ systematics in terrestrial uranium-bearing minerals. Science 335, 1610–1640.

Hillaire-Marcel, C., Carro, O., Casanova, J., 1986. ^{14}C and Th/U dating of Pleistocene and Holocene stromatolites from East African paleolakes. Quat. Res. 25, 312–329.

Hogg, A.G., Hua, Q., Blackwell, P.G., Niu, M., Buck, C.E., Guilderson, T.P., Heaton, T.J., Palmer, J.G., Reimer, P.J., Reimer, R.W., Turney, C.S.M., Zimmermann, S.R.H., 2013. SHCal13 southern hemisphere calibration, 0-50,000 years cal BP. Radiocarbon 55, 1889–1903.

Hora, J.M., Singer, B.S., Jicha, B.R., Beard, B.L., Johnson, C.M., de Silva, S., Salisbury, M., 2010. Volcanic biotite-sanidine $^{40}Ar/^{39}Ar$ age discordances reflect Ar partitioning and pre-eruption closure in biotite. Geology 38, 923–926.

Kelley, S., 2002. Excess argon in K-Ar and Ar-Ar geochronology. Chem. Geol. 188, 1–22.

Lippolt, H.J., Troesch, M., Hess, J.C., 1990. Excess argon and dating of Quaternary Eifel volcanism, IV. Common argon with high and lower-than-atmospheric $^{40}Ar/^{36}Ar$ ratios in phonolitic rocks, East Eifel, F.R.G. Earth Planet Sci. Lett. 101, 19–33.

Liutkus-Pierce, C.M., Zimmer, B.W., Carmichael, S.K., McIntosh, W., Deino, A., Hewitt, S.M., McGinnis, K.J., Hartney, T., Brett, J., Mana, S., Deocampo, D., Richmond, B.G., Hatala, K., Harcourt-Smith, W., Pobiner, B., Metallo, A., Rossi, V., 2016. Radioisotopic age, formation, and preservation of Late Pleistocene human footprints at Engare Sero, Tanzania. Palaeogeogr. Palaeoclimatol. Palaeoecol. 463, 68–82.

Mastrolorenzo, G., Palladino, D.M., Vecchio, G., Taddeucci, J., 2002. The 472 AD Pollena eruption of Somma–Vesuvius (Italy) and its environmental impact at the end of Roman Empire. J. Volcanol. Geoth. Res. 113, 19–36.

McDougall, I., Harrison, T.M., 1999. Geochronology and Thermochronology by the $^{40}Ar/^{39}Ar$ Method, second ed. Oxford University Press, Oxford.

Mollex, G., Füri, E., Burnard, P., Zimmermann, L., Chazot, G., Kazimoto, E.O., Marty, B., France, L., 2018. Tracing helium isotope compositions from mantle source to fumaroles at Pldoinyo Lengai volcano, Tanzania. Chem. Geol. 480, 66–74.

Principe, C., Tanguy, J.C., Arrighi, S., Paiotti, A., Le Goff, M., Zoppi, U., 2004. Chronology of Vesuvius' activity from A.D. 79 to 1631 based on archeomegnetism of lavas and historical sources. Bull. Volcanol. 66, 703–724.

Renne, P.R., 1995. Excess ^{40}Ar in biotite and hornblende from the Noril'sk 1 intrusion, Siberia: implications for the age of the Siberian Traps. Earth Planet Sci. Lett. 131, 165–176.

Rolandi, G., Munno, R., Postiglione, I., 2004. The AD 472 eruption of the Somma volcano. J. Volcanol. Geoth. Res. 129, 291–319.

Rosi, M., Santacroce, R., 1983. The A.D. 472 "Pollena" eruption: volcanological and petrological data for this poorly-known, Plinian-type event at Vesuvius. J. Volcanol. Geoth. Res. 17, 249–271.

Rosi, M., Santacroce, R., 1984. Volcanic hazard assessment in the Phlegraean Fields: a contribution based on stratigraphic and historical data. Bull. Volcanol. 47, 359–370.

Russell, J.K., Dipple, G.M., Lang, J.R., Lueck, B., 1999. Major-element discrmination of titanian andradite from magmatic and hydrothermal environments : an example from the Canadian Cordillera. Eur. J. Mineral 11, 919–935.

Santacroce, R., Cioni, R., Marianelli, P., Sbrana, A., Sulpizio, R., Zanchetta, G., Donahue, D.J., Joron, J.L., 2008. Age and whole rock-glass compositions of proximal pyroclastics from the major explosive eruptions of Somma-Vesuvius: a review as a tool for distal tephrostratigraphy. J. Volcanol. Geoth. Res. 177, 1–18.

Scheibner, B., Wörner, G., Civetta, L., Simon, K., Kronz, A., 2007. Rare earth element fractionation in magmatic Ca-rich garnets. Contrib. Mineral. Petrol. 154, 55–74.

Scheibner, B., Heumann, A., Wörner, G., Civetta, L., 2008. Crustal residence times of explosive phonolite magmas: U-Th ages of magmatic Ca-garnets of Mt. Somma-Vesuvius (Italy). Earth Planet Sci. Lett. 276, 293–301.

Schmitt, A.K., 2006. Laacher See revisited: high-spatial-resolution zircon dating indicates rapid formation of a zoned magma chamber. Geology 34, 597–600.

Seman, S., Stockli, D.F., McLean, N.M., 2017. U-Pb geochronology of grossular-andradite garnet. Chem. Geol. 460, 106–116.

Stoppa, F., Lavecchia, G., 1992. Late Pleistocene ultra-alkaline magmatic activity in the Umbria-Latium region (Italy): an overview. J. Volcanol. Geoth. Res. 52, 277–293.

Stoppa, F., Woolley, A.R., Cundari, A., 2002. Extension of the melilite-carbonatite province in the Apennines of Italy: the kamafugite of Grotto del Cervo, Abruzzo. Mineral. Mag. 66, 555–574.

Stuiver, M., Reimer, P.J., Reimer, R.W., 2018. CALIB 7.1 [WWW program] at http://calib.org.
Sulpizio, R., Mele, D., Dellino, P., Volpe, L.L., 2005. A complex, Subplinian-type eruption from low-viscosity, phonolitic to tephri-phonolitic magma: the AD 472 (Pollena) eruption of Somma-Vesuvius, Italy. Bull. Volcanol. 67, 743–767.
Sulpizio, R., Mele, D., Dellino, P., La Volpe, L., 2007. Deposits and physical properties of pyroclastic density currents during complex subplinian eruptions: the AD 472 (Pollena) eruption of Somma-Vesuvius, Italy. Sedimentology 54, 607–635.
Teague, A.J., Seward, T.M., Harrison, D., 2008. Mantle source for Oldoinyo Lengai carbonatites: evidence from helium isotopes in fumarole gases. J. Volcanol. Geoth. Res. 175, 386–390.
Vermeesch, P., 2018. IsoplotR: a free and open toolbox for geochronology. Geoscience Frontiers 9, 1479–1493.
Zhang, C., Giere, R., Stünitz, H., Brack, P., Ulmer, P., 2001. Garnet-quartz intergrowth in granitic pegamtites from Bergell and Adamello. Schweizer Mineralogische und Petrographische Mitteilungen 81, 89–113.